CD99-like 2 (CD99L2)-deficient mice are defective in the acute inflammatory response

Nakisha S. Rutledge[1], **Evan W. Weber**[1], **Ryan Winger**[1], **Warren G. Tourtellotte**[1,2], **Seong Hoe Park**[3], and **William A. Muller**[1,4]

[1]Department of Pathology, Northwestern University Feinberg School of Medicine, 303 East Chicago Avenue, Chicago, IL 60611

[2]Department of Neurology, Northwestern University Feinberg School of Medicine, 303 East Chicago Avenue, Chicago, IL 60611

[3]Transplantation Research Institute, MRC, Seoul National University College of Medicine Seoul, South Korea

Abstract

CD99-Like 2 (CD99L2) is a Type I glycoprotein expressed on leukocytes and endothelial cells as well as other cell types. It is related to CD99, although it shows only 38% sequence identity. CD99L2 has been shown to play a role in leukocyte extravasation in mice under various inflammatory conditions using anti-CD99L2 antibodies and, in one case by targeted deletion of CD99L2. We report here studies on an independently made CD99L2 "knockout mouse" that extend our knowledge of the role of CD99L2 in inflammation. CD99L2 deficiency did not affect the total or relative numbers of circulating leukocyte subsets, red blood cells, or platelets. Neither did CD99L2 deficiency affect the expression of ICAM-1, PECAM, or CD99 on endothelial cells. Mice lacking CD99L2 had a defective inflammatory response in the thioglycollate peritonitis model with a greater than 80% block in neutrophil infiltration and a nearly complete block in monocyte emigration into the peritoneal cavity measured 16 hours after the inflammatory challenge. The mice will be a useful resource to study the role of CD99L2 in various acute and chronic inflammatory diseases.

Keywords

CD99L2; inflammation; adhesion molecule; leukocyte; endothelium; knockout mouse

---

[4]Corresponding Author: William A. Muller, MD, PhD, Department of Pathology, Northwestern University Feinberg School of Medicine, 303 East Chicago Avenue, Chicago, IL 60611, wamuller@northwestern.edu.

Introduction

Leukocyte extravasation involves a series of adhesive and signaling interactions between leukocytes and endothelial cells (Butcher, 1991; Ley et al., 2007; Muller, 2011). These interactions allow leukocytes to form increasingly firm attachment to the endothelium at sites of inflammation as they undergo fast rolling then slow rolling, adhesion, and locomotion (intraluminal crawling) prior to leaving the vessel (Ley et al., 2007; Muller, 2011, 2015). These steps are all critical for leukocyte extravasation, but they are reversible. Most leukocytes that enter a postcapillary venule at the site of inflammation do not roll; most leukocytes that roll don't adhere, and most that adhere don't extravasate (Sumagin et al., 2010). However, once leukocytes make the commitment to cross the endothelium into the tissue, with notable exceptions (Woodfin et al., 2011), they don't go back—at least not as the same type of cell. Thus, diapedesis or transendothelial migration (TEM) is a logical process to study if one hopes to control an ongoing inflammatory response (Muller, 2009, 2011).

CD99L2 is a Type I glycoprotein expressed on leukocytes and endothelial cells as well as other cell types (Bixel et al., 2007; Schenkel et al., 2007; Suh et al., 2003). It has been shown to play a role in extravasation of neutrophils, monocytes, and T lymphocytes in mice under various inflammatory conditions (Bixel et al., 2010; Bixel et al., 2007; Schenkel et al., 2007; Seelige et al., 2013). However, despite its non-redundant role in the inflammatory response, there have been very few studies of CD99L2 in inflammation (only four in the literature thus far) and it has been studied in different mouse strains and under different inflammatory conditions by the two labs that have studied it. Most of the published studies used polyclonal antibodies generated against murine CD99 (Bixel et al., 2010; Bixel et al., 2007; Schenkel et al., 2007). There has been one brief report of targeted deletion of CD99L2 in the C57Bl/6 background (Seelige et al., 2013), in which there was an approximately 20–40% reduction in neutrophil or T cell emigration depending on the inflammatory model. However, the expression of other molecules relevant to transmigration on either leukocytes or endothelial cells in those CD99L2 "knockout" mice were not reported and the effect of CD99L2 deficiency on inflammation was only studied for 4–5 hours.

In order to further study the role of CD99L2 in the inflammatory response, we developed an independent CD99L2-deficient mouse and characterized expression of relevant adhesion molecules on its leukocytes and endothelial cells. We studied inflammation in these mice under conditions not examined in the previous report of CD99L2 knockout (Seelige et al., 2013). Specifically, we studied the effect of CD99L2 deletion in mice of the FVB/n strain and studied examined the effects on monocytes as well as neutrophils after 16 hours of inflammatory challenge. Having CD99L2-deficient mice in both C57Bl/6 and FVB/n strains will allow direct comparison of the effect of strain difference on the role of CD99L2 in leukocyte transendothelial migration.

Materials and Methods

Generating CD99L2 KO mice

A homologous recombination targeting construct was generated containing two homology arms and a positive selection marker PGK-Neo (Tourtellotte and Milbrandt, 1998). To minimize potential promoter interference PGK-Neo was inserted in the anti-sense orientation. Mouse genomic DNA was manipulated to substitute PGK-Neo for the entire first coding exon of CD99L2 (124 nt) which included the translation start codon and a portion of intron 1 (990 nt) (net substitution of 1114 nt; nt 225–1338, Genbank NC_000086.7 of CD99L2). The targeting construct was electroporated into ES cells and genomic DNA isolated from G418-resistant clones was screened by PCR and Southern blotting for specific homologous recombination. Targeted ES cells were injected into C57BL/6J blastocysts and chimeric mice were generated and mated to C57BL/6J female mice to generate germline heterozygous CD99L2+/− mice. Germline CD99L2+/− heterozygous mice were initially inbred with isogenic C57BL/6J mice. The mice were genotyped using unique primers in the forward direction and a common primer in the reverse direction: WT_{for}: 5'-TTAGCGAAATAATCAGATCC-3', Rev: 5'-CACTGAAAGGTTCTATAAGTGACAT-3' and KO_{for}: 5'-GAAGGAGCAAAGCTGCTATT-3' (Fig. 1A). Standard PCR conditions were used with the addition of 1.25% DMSO and primer annealing temperature of 60°C.

Animal husbandry

All procedures were approved by the Institutional Animal Use and Care Committee of the Feinberg School of Medicine. Mice were maintained under standard barrier conditions in the vivarium at Northwestern University Feinberg School of Medicine, an AALAC-accredited facility, under the care of trained veterinary staff. Animals were given *ad libidum* access to food and water. Genotyping was performed by standard tail-tipping methods using the primers listed above. For the thioglycollate experiments, CD99L2-deficient mice were backcrossed into the FVB/n strain for 9 generations.

Complete Blood Counts

Blood was collected from anesthetized mice in heparinized syringes by cardiac puncture. Automated complete blood counting was performed using a Hemavet, model HV950FS (Drew Scientific, Miami Lakes, FL) calibrated for mouse blood.

Immunoperoxidase Histochemistry

Organs from wild-type and CD99L2$^{-/-}$ mice were snap frozen in Optimal Cutting Temperature (OCT) embedding media (Sakura Finetek USA, Torrence, CA). Frozen sections 12 μm thick were cut on a Leica CM 1850 cryostat and picked up on poly-L-lysine coated masked glass slides (Schenkel et al., 2007). Slides were dehydrated under vacuum at room temperature, blocked in 5% serum of the species of the secondary antibody in PBS, then stained with primary antibodies at room temperature for 30 minutes. Primary antibodies were monoclonal rat anti-ICAM-1 (clone YN1/1.7.4, Abcam, Cambridge,MA), rat anti-PECAM-1 (clone 390, Millipore, Temecula, CA), and rat anti-CD99 (clone 3F11(Watson et

al., 2015)), as well as rabbit polyclonal anti-mouse CD99L2 (a generous gift from Dr. Dietmar Vestweber, Muenster, Germany). Following extensive washing in PBS + 0.1% BSA, HRP-conjugated secondary antibodies were applied for an additional 30 minutes. Slides were then washed, exposed to 3,3'-diaminobenzidine (1 mg/ml) and H_2O_2 (0.03%) in PBS for several minutes, then rinsed extensively in PBS. Slides were counterstained with Meyer's Hematoxylin, dehydrated in graded alcohols and xylene, then mounted for microscopic viewing. Images were taken using a SPOT model 2.3.1 camera mounted to a Nikon microscope.

Flow cytometry

Mice were sacrificed by CO_2 and blood was collected via cardiac puncture using heparinized syringes. RBC were lysed using BD Pharm lyse™ (BD Bioscience, San Jose, CA) per manufacturer's instructions. Cells were washed 2–3 times using complete Hanks Buffered Salt Solution (HBSS containing 10% FBS + 2 mM EDTA) via resuspension and centrifugation at 1200 RPM for 5 minutes at 4°C. Cells were then resuspended in appropriate volume of FACS buffer (DPBS without Ca^{++}/Mg^{++} containing 2% FBS and 2mM EDTA). Cells were blocked with anti-CD16/32 mAb (FcRIIB/FcRIIIA, clone 2.4G2; BD Bioscience) for 15 min at 4°C to avoid nonspecific staining. Cells were washed via resuspension and centrifugation at 1700 RPM for 3 min at 4°C followed by incubation with VID dye (Invitrogen) for 15 min at 4°C in the dark for live/dead discrimination. Cells were washed and incubated with antibodies (eBioscience) against cell surface markers CD45, Ly6G/Ly6c (Gr-1), CD11b, CD3, CD19, PECAM and CD99 for 30 min at 4°C in the dark. Cells were then washed and resuspended in appropriate volume of FACS buffer for immediate analysis. For control staining, unstained cells and OneComp eBeads (eBioscience) were used for single-color compensation. ArC™ amine reactive compensation beads (Invitrogen) that are specifically designed for use with live/dead cell staining were used as additional controls. Data were acquired on a BD LSRII flow cytometer (BD Biosciences) and analyzed with FlowJo software (Tree Star, Ashland, OR).

Thioglycollate Peritonitis

Brewer Thioglycollate Medium powder was purchased from Difco (Detroit, Mi). Sterile thioglycollate broth (4% in water) was stored at room temperature protected from light. The thioglycollate peritonitis assay was performed as previously described (Bogen et al., 1994; Liao et al., 1997; Liao et al., 1999; Schenkel et al., 2004; Schenkel et al., 2007). Briefly, one (1) ml of 4% thioglycollate broth was injected intraperitoneally into mice sixteen (16) hours prior to sacrifice. Mice were killed by exposure to CO_2. Peripheral blood was harvested by cardiac puncture into heparinized syringes. The peritoneal cavity was lavaged with 5ml of 10 mM EDTA in Hanks' Buffered Saline Solution without divalent cations. Total peritoneal cell counts were performed using a hemacytometer. Differential counts were performed on cytospins stained with modified Wright-Giemsa stain (Hema 3, Fisher Scientific, Kalamazoo, MI). Peripheral blood was diluted in Turk's Solution and counted using a hemacytometer.

Statistics

Blood counts between wild-type and CD99L2 knockout mice were compared by Student's two- tailed t test. Thioglycollate data were analyzed using ANOVA.

Results

A construct containing a neomycin resistance cassette was used to target exon 1 of CD99L2 by conventional homologous recombination technologies (Fig. 1a). PCR primers were designed to distinguish the wild-type and knockout alleles (Fig. 1b). For purposes of comparison with our previous work (Dufour et al., 2008), homozygous deficient mice were backcrossed over nine times into the FVB/n strain. Mice deficient for CD99L2 appeared normal, developed and gained weight normally, and had normal lifespans in conventional barrier housing. They showed no tendency to become ill or have difficulty healing wounds. Necropsy of healthy mice did not reveal any gross abnormalities of internal organs. (Data not shown.) Complete blood counts revealed no significant differences in absolute numbers or percent of total circulating elements or subtypes of white blood cells, numbers or size of red cells, or platelet counts between knockouts and age-matched wild-type controls (Table I).

Using a polyclonal antibody against murine CD99L2, we verified that CD99L2 protein expression was absent from mouse endothelial cells (Fig. 2) and mouse leukocytes (not shown). Immunoperoxidase histochemistry of mouse tissues revealed intense staining of PECAM-1 and ICAM-1 on all levels of endothelium in both wild-type and CD99L2 knockout mice as well as weak but consistent staining of CD99 on both genotypes. Notably, there was no change in expression of CD99, PECAM, or ICAM-1 on endothelium of CD99L2 knockout mice compared to wild-type (Fig. 2). Similar results were seen by immunofluorescence (not shown). CD99L2 stained endothelium of wild-type mice intensely, but no staining was seen in the knockouts, as expected.

Similarly, the levels of CD99, PECAM (Fig. 3), and CD18 (not shown) on leukocytes from CD99L2 knockout mice were identical to those of age- and sex-matched wild-type FVB/n controls (Fig. 3). In particular, while neutrophils, monocytes, T cells and B cells expressed different levels of PECAM and CD99 from each other, there was no difference in the amount expressed by those leukocyte subsets from wild-type and CD99L2 knockout mice.

We compared the inflammatory response of wild-type and CD99L2$^{-/-}$ mice in the thioglycollate peritonitis model of sterile inflammation (Bogen et al., 1994; Liao et al., 1997; Liao et al., 1999; Schenkel et al., 2004; Schenkel et al., 2007). Sixteen hours after intraperitoneal injection of 4% thioglycollate broth, mice were sacrificed and peritoneal cavities were lavaged with 5 ml of HBSS containing 10 mM EDTA as previously described (Bogen et al., 1994; Liao et al., 1997; Liao et al., 1999; Schenkel et al., 2004; Schenkel et al., 2007). This timing allowed us to determine the effect of CD99L2 deficiency on both neutrophils and monocytes. Peripheral blood was recovered by cardiac puncture into heparinized syringes. Absolute and differential counts of recovered cells were performed. The peritoneal cavities of resting CD99L2$^{-/-}$ mice contained normal numbers of macrophages, lymphocytes, and mast cells (Fig. 4). However, the response of both PMN and

monocytes was markedly diminished in CD99L2$^{-/-}$ mice (Fig. 4). In three independent experiments, the response of neutrophils was blocked by an average of 83%. The influx of monocytes was reduced almost to baseline levels (Fig. 4). Peripheral blood white cell counts at the time of harvest were not significantly different among the groups, indicating that the reduction in the influx of leukocytes into the peritoneal cavity of CD99L2$^{-/-}$ mice was not due to reduced numbers of leukocytes in the circulation (Data not shown.)

Discussion

Our data show that in the constitutive absence of CD99L2, CD99 levels on endothelial cells (Fig. 2) and leukocytes (Fig. 3) do not change from wild-type levels. CD99 does not increase to compensate for absence of CD99L2. A recent paper by Nam *et al.* (Nam et al., 2013) showed that in mouse cells CD99 and CD99L2 interact via their cytoplasmic domains during their biosynthesis. CD99 helps CD99L2 get to the cell surface, and levels of CD99L2 were decreased in cells lacking CD99. Even though the authors did not find the reciprocal relationship to be true, it was important to make sure that knockout of CD99L2 did not cause levels of CD99 to decrease, as this would be an alternative explanation for the defect in transendothelial migration in the CD99L2 knockout mice. Therefore, it is important that CD99 levels did not decrease in the absence of CD99L2. Other molecules important for leukocyte adhesion to and migration across endothelial cells also did not change (Figs. 2, 3), indicating that the defect in inflammation in our CD99L2 knockout mice, and presumably as well as in an independent knockout (Seelige et al., 2013) is due to absence of CD99L2.

Our previous studies on CD99L2 employed polyclonal antibodies raised in rabbits or rats against recombinant murine CD99L2 purified from transfected mouse L cells (Schenkel et al., 2007). In the thioglycollate peritonitis model in wild-type FVB/n mice, these antibodies still blocked influx of neutrophils by > 65% compared to preimmune controls 18 hours after antibody administration. Monocyte/macrophage levels were blocked almost to baseline levels. Using our CD99L2 knockout mice backcrossed into the FVB/n strain, in the same thioglycollate peritonitis model, neutrophil influx is diminished by > 80% compared to wild-type littermates and monocyte levels in the peritoneal cavity were at baseline levels. Thus, in the FVB/n strain, we get a similar decrease in inflammation whether we interfere with CD99L2 function using antibodies or genetic deletion.

The Vestweber group has also studied CD99L2 function in mice using both rabbit polyclonal antibody generated against a mouse CD99L2-Fc fusion protein (Bixel et al., 2007) and genetic deletion of CD99L2 (Seelige et al., 2013). In general, our results are similar. Using antibody in the thioglycollate peritonitis model they found a 69% reduction of PMN emigration at 4 hours (Bixel et al., 2007); we found a 65% reduction in PMN emigration at 18 hours (Schenkel et al., 2007). Using CD99L2 knockout mice in the thioglycollate peritonitis model, they found a 43% reduction of PMN emigration at 4 hours (Seelige et al., 2013); we found a 83% reduction in PMN emigration at 16 hours.

However, the studies we report here add important additional information. We show that in the knockout as well as antibody-treated mice, monocyte migration is reduced to baseline levels. More important, we show that in the absence of CD99L2, levels of other molecules

critical to leukocyte adhesion and transmigration (e.g. ICAM-1, PECAM, and CD99) are not altered on leukocytes or endothelial cells. This shows that the defect in leukocyte emigration is due to absence of CD99L2, and not diminished levels of one or more of these other molecules.

Acknowledgments

References

Bixel MG, Li H, Petri B, Khandoga AG, Khandoga A, Zarbock A, Wolburg-Buchholz K, Wolburg H, Sorokin L, Zeuschner D, et al. CD99 and CD99L2 act at the same site as, but independently of, PECAM-1 during leukocyte diapedesis. Blood. 2010; 116:1172–1184. [PubMed: 20479283]

Bixel MG, Petri B, Khandoga AG, Khandoga A, Wolburg-Buchholz K, Wolburg H, Marz S, Krombach F, Vestweber D. A CD99-related antigen on endothelial cells mediates neutrophil, but not lymphocyte extravasation in vivo. Blood. 2007; 109:5327–5336. [PubMed: 17344467]

Bogen S, Pak J, Garifallou M, Deng X, Muller WA. Monoclonal antibody to murine PECAM-1 [CD31] blocks acute inflammation in vivo. J Exp Med. 1994; 179:1059–1064. [PubMed: 8113674]

Butcher EC. Leukocyte-endothelial cell recognition: three (or more) steps to specificity and diversity. Cell. 1991; 67:1033–1036. [PubMed: 1760836]

Dufour EM, Deroche A, Bae Y, Muller WA. CD99 is essential for leukocyte diapedesis in vivo. Cell Commun Adhes. 2008; 15:351–363. [PubMed: 18923973]

Ley K, Laudanna C, Cybulsky MI, Nourshargh S. Getting to the site of inflammation: the leukocyte adhesion cascade updated. Nat Rev Immunol. 2007; 7:678–689. [PubMed: 17717539]

Liao F, Ali J, Greene T, Muller WA. Soluble domain 1 of platelet-endothelial cell adhesion molecule (PECAM) is sufficient to block transendothelial migration in vitro and in vivo. J Exp Med. 1997; 185:1349–1357. [PubMed: 9104821]

Liao F, Schenkel AR, Muller WA. Transgenic mice expressing different levels of soluble platelet/ endothelial cell adhesion molecule-IgG display distinct inflammatory phenotypes. J Immunol. 1999; 163:5640–5648. [PubMed: 10553094]

Muller WA. Mechanisms of transendothelial migration of leukocytes. Circ Res. 2009; 105:223–230. [PubMed: 19644057]

Muller WA. Mechanisms of leukocyte transendothelial migration. Annu Rev Pathol. 2011; 6:323–344. [PubMed: 21073340]

Muller WA. The regulation of transendothelial migration: new knowledge and new questions. Cardiovasc Res. 2015

Nam G, Lee YK, Lee HY, Ma MJ, Araki M, Araki K, Lee S, Lee IS, Choi EY. Interaction of CD99 with Its Paralog CD99L2 Positively Regulates CD99L2 Trafficking to Cell Surfaces. J Immunol. 2013; 19:5730–5742. [PubMed: 24133166]

Schenkel AR, Chew TW, Muller WA. Platelet endothelial cell adhesion molecule deficiency or blockade significantly reduces leukocyte emigration in a majority of mouse strains. J Immunol. 2004; 173:6403–6408. [PubMed: 15528380]

Schenkel AR, Dufour EM, Chew TW, Sorg E, Muller WA. The Murine CD99-Related Molecule CD99-Like 2 (CD99L2) Is an Adhesion Molecule Involved in the Inflammatory Response. Cell Commun Adhes. 2007; 14:227–237. [PubMed: 18163232]

Seelige R, Natsch C, Marz S, Jing D, Frye M, Butz S, Vestweber D. Cutting edge: Endothelial-specific gene ablation of CD99L2 impairs leukocyte extravasation in vivo. J Immunol. 2013; 190:892–896. [PubMed: 23293350]

Suh YH, Shin YK, Kook MC, Oh KI, Park WS, Kim SH, Lee IS, Park HJ, Huh TL, Park SH. Cloning, genomic organization, alternative transcripts and expression analysis of CD99L2, a novel paralog

of human CD99, and identification of evolutionary conserved motifs. Gene. 2003; 307:63–76. [PubMed: 12706889]

Sumagin R, Prizant H, Lomakina E, Waugh RE, Sarelius IH. LFA-1 and Mac-1 define characteristically different intralumenal crawling and emigration patterns for monocytes and neutrophils in situ. J Immunol. 2010; 185:7057–7066. [PubMed: 21037096]

Tourtellotte WG, Milbrandt J. Sensory ataxia and muscle spindle agenesis in mice lacking the transcription factor Egr3. Nat Genet. 1998; 20:87–91. [PubMed: 9731539]

Watson RL, Buck J, Levin LR, Winger RC, Wang J, Arase H, Muller WA. Endothelial CD99 signals through soluble adenylyl cyclase and PKA to regulate leukocyte transendothelial migration. The Journal of experimental medicine. 2015; 212:1021–1041. [PubMed: 26101266]

Woodfin A, Voisin MB, Beyrau M, Colom B, Caille D, Diapouli FM, Nash GB, Chavakis T, Albelda SM, Rainger GE, et al. The junctional adhesion molecule JAM-C regulates polarized transendothelial migration of neutrophils in vivo. Nat Immunol. 2011; 12:761–769. [PubMed: 21706006]
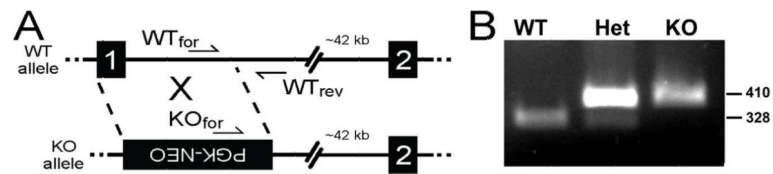
Figure 1. Targeting scheme for and verification of deletion of CD99L2 by homologous recombination

See Materials and Methods for details. A. Two forward primers and a common reverse primer were designed for a multiplex PCR system. Black boxes with numbers denote exons. PGK-NEO cassette in the inverse orientation is shown in the knockout allele. B. PCR results from wild-type, heterozygous, and CD99L2-deficient mice. Numbers at the right indicate the molecular size in base pairs.
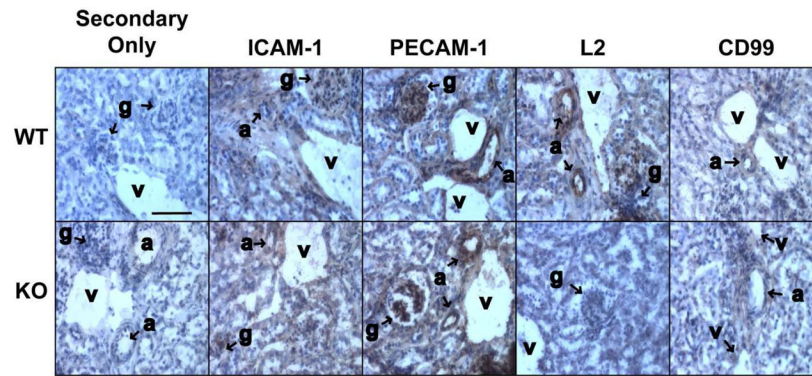
Figure 2. Expression of relevant endothelial cell adhesion molecules by CD99L2-deficient mice
Frozen sections of mouse kidney from wild-type (WT) or CD99-deficient (KO) mice were incubated with antibodies against ICAM-1, PECAM-1, CD99L2 (L2), or CD99 then with HRP-conjugated secondary antibody or Secondary antibody alone (negative control). After development of peroxidase reaction product, slides were counterstained with hematoxylin. Brown reaction product is seen on endothelial cells of all levels: arterioles (a), glomerular capillaries (g), venules (v), and peritubular capillaries. Scale bar = 80 μm.
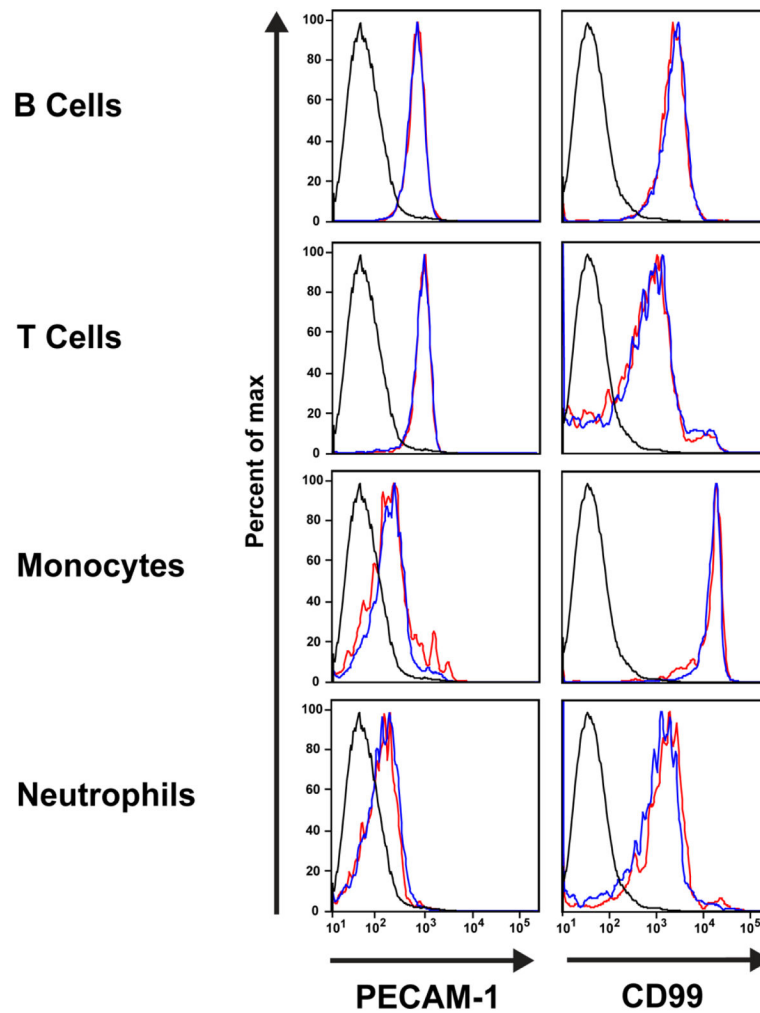
Figure 3. Expression of PECAM and CD99 is similar on leukocytes from wild-type and CD99L2$^{-/-}$ mice

Flow cytometric profiles of PECAM and CD99 on leukocytes gated by forward and side scatter as well as cell-specific markers. At least 100,000 events were recorded per sample. Details of the full surface marker panel can be found in Materials and Methods. Black histogram = unstained negative control; blue histogram = wild-type; red histogram = CD99L2$^{-/-}$.
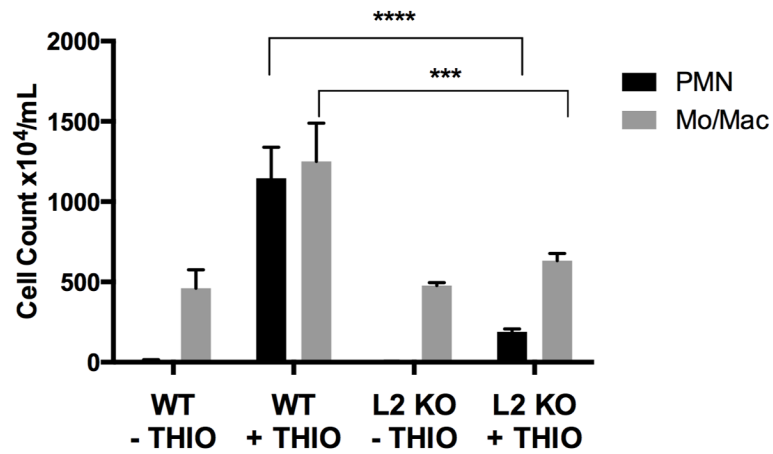
Figure 4. CD99L2⁻/⁻ mice have defective acute inflammatory response

Age-and sex-matched wild-type (**WT**) or CD99L2 knockout (**L2 KO**) mice were left untreated for baseline measurements (**– THIO**) or received an intraperitoneal injection of thioglycollate (**+ THIO**) 16 hours prior to sacrifice and harvest of peritoneal cells. Very few PMN were present in the unstimulated peritoneal cavity of unstimulated mice. Black bars = PMN; grey bars = Monocytes. Mean ± SEM of 3 independent experiments *** $p<0.001$; **** $p< 0.0001$ by two-way ANOVA.

Table I

Circulating Blood Cell Counts for Wild-Type and CD99L2-Deficient Mice

	Wild Type	CD99L2$^{-/-}$	
	Mean ± SD	Mean ± SD	p value
WBC (K/uL)	7.70 ± 3.31	6.48 ± 2.30	0.48
NE# (K/uL)	1.69 ± 0.68	1.50 ± 0.44	0.58
LY# (K/uL)	5.59 ± 2.65	4.70 ± 2.01	0.53
MO# (K/uL)	0.28 ± 0.23	0.21 ± 0.08	0.53
EO# (K/uL)	0.12 ± 0.14	0.06 ± 0.06	0.33
BA# (K/uL)	0.02 ± 0.03	0.02 ± 0.02	0.91
NE (%)	23.23 ± 6.61	25.14 ± 9.83	0.70
LY (%)	71.11 ± 5.17	70.27 ± 9.32	0.85
MO (%)	3.48 ± 3.42	3.29 ± 0.88	0.90
EO (%)	1.85 ± 2.11	0.99 ± 1.19	0.41
BA (%)	0.34 ± 0.42	0.31 ± 0.39	0.90
RBC (M/uL)	7.23 ± 1.31	8.04 ± 1.14	0.28
HB (g/uL)	9.32 ± 1.43	10.25 ± 1.46	0.29
HCT (%)	30.90 ± 5.71	33.83 ± 5.11	0.37
MCV (fL)	42.72 ± 0.66	42.02 ± 0.73	0.11
MCH (Pg)	12.97 ± 0.48	12.75 ± 0.55	0.49
MCHC (g/dL)	30.32 ± 1.46	30.37 ± 1.13	0.95

Freshly-isolated heparinized blood from six CD99L2-deficient mice in the C57Bl/6 strain background and six age- and sex-matched wild-type littermates was analyzed as described in Materials & Methods. Data are expressed as mean ± standard deviation. No significant differences were found in any of the parameters by t-test.

WBC=white blood cells; NE= neutrophils; LY=lymphocytes; MO=monocytes; EO=eosinophils; BA=basophils; RBC=red blood cells; HB=hemoglobin; HCT= hematocrit; MCV= mean corpuscular red blood cell volume; MCH= mean corpuscular hemoglobin; MCHC= mean corpuscular red cell hemoglobin concentration.